A Comprehensive Study on the Influence of Proximity Effects on Electromagnetic Transients in Power Cables

Utkarsh R. Patel and Piero Triverio

***Abstract*—In this paper, we present a comprehensive study on the influence of proximity effects on electromagnetic transients in underground power cables. Existing simulators for electromagnetic transients (EMT) neglect proximity effects when computing cable parameters. It has been demonstrated that, in some scenarios, this approximation can result in significant errors on the predicted transients. The goal of this study is to identify the scenarios where proximity effects must be taken into account, and the error that one may incur if such effects are neglected. The study is performed using the recently-proposed MoM-SO method for the determination of cable resistance and inductance. MoM-SO accurately predicts skin, proximity, and ground effects over the frequency range of interest for transient analyses, with an accuracy comparable to time-consuming finite element calculations. The study considers cables of different type and geometry under multiple excitation scenarios. Results elucidate the role of proximity effects on the response of typical power cables and are finally summarized into guidelines to help power engineers model power cables accurately.**

***Keywords*: Series impedance computation, wideband cable modeling, underground cables, electromagnetic transients, proximity effects.**

I. Introduction and Motivation

Electromagnetic transients induced by phenomena such as faults, lightning, and breakers operation are a major concern for power grid operators, and must be accurately predicted using electromagnetic transient (EMT) simulators during grid planning. These analyses can be performed only if accurate models are readily available for all parts of the system, including underground cables that are increasingly used by the power industry. Most EMT tools on the market use analytic formulas [1] to model power cables. Unfortunately, such formulas neglect proximity effects that may develop when core conductors or sheaths are close to each other. While, for certain cable configurations, this approximation is well-posed, recent works [2], [3], [4], [5] demonstrated that neglecting proximity may lead to erroneous transient predictions in commonly-used cable configurations, such as flat and pipe-type formations.

The goal of this study is to thoroughly investigate proximity effects on power cables, and elucidate their influence on transient scenarios. We consider two among the most common formations for three-phase power cables (flat formation and pipe-type), and we parametrize the analysis with respect to cable geometry and material parameters. Different excitation conditions are investigated in order to understand how proximity effects affect the different modes that can propagate along a cable, such as the core-sheath mode and the intersheath mode. The error caused by neglecting proximity effects on transient waveforms and power loss is quantified and thoroughly analysed. Finally, guidelines are proposed to assist power engineers in understanding when proximity effects must be taken into account, and when they can be neglected with an acceptable accuracy loss.

In this study, cable parameters are computed with the recently-proposed MoM-SO method [6], [7], [8]. In comparison to analytic formulas employed by most EMT solvers, MoM-SO accurately predicts proximity, and ground effects, in addition to skin effect. MoM-SO was demonstrated [6], [7], [8] to be as accurate as other proximity-aware methods, such as the finite element method (FEM), conductor partitioning or other general-purpose electromagnetic solvers [9], [10], [11]. However, while the FEM analysis of a single power cable can take several hours, MoM-SO requires only a few seconds.

II. MoM-SO

In this Section, we briefly review the MoM-SO method which will be used to investigate proximity effects in power cables. MoM-SO computes the per-unit-length resistance and inductance of cables made by solid and hollow (tubular) conductors in arbitrary position [6], [7]. The conductors can be in air or buried into ground, which is modelled as a lossy conductor with conductivity σ_g. Conductors can be in direct contact with the surrounding ground, or can be placed in a hole dug in ground [8]. A simple configuration, which will be used to explain how MoM-SO works, is depicted in the left panel of Fig. 1. This configuration consists of two solid conductors placed into a hole dug in a conductive ground at a certain depth. In order to calculate the cable impedance, MoM-SO first represents the electric field on the boundary of

This work was supported in part by the KPN project "Electromagnetic transients in future power systems" (ref. 207160/E20) financed by the Norwegian Research Council (RENERGI programme) and by a consortium of industry partners led by SINTEF Energy Research: DONG Energy, EdF, EirGrid, Hafslund Nett, National Grid, Nexans Norway, RTE, Siemens Wind Power, Statnett, Statkraft, and Vestas Wind Systems.

U. R. Patel and P. Triverio are with the Edward S. Rogers Sr. Department of Electrical and Computer Engineering, University of Toronto, Toronto, M5S 3G4 Canada (email: utkarsh.patel@mail.utoronto.ca, piero.triverio@utoronto.ca).

Paper submitted to the International Conference on Power Systems Transients (IPST2015) in Cavtat, Croatia June 15-18, 2015.

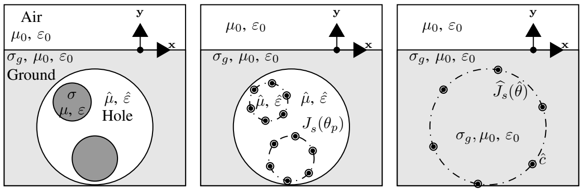

Fig. 1. **Left Panel:** Sample cross-section of the cable. The cable is made up of 2 solid conductors, which are placed inside a hole buried in ground. Conductive media are shown in gray, while dielectric media are shown in white. **Center panel:** cross-section of the cable after applying the equivalence theorem on the conductors. Equivalent currents $J_s(\theta_p)$ are introduced on the boundary of the conductors. **Right panel:** Cross-section of the cable after applying the equivalence theorem to the cable-hole system. An equivalent current $\widehat{J}_s(\hat{\theta})$ is introduced on the hole boundary $\hat{c}$.

each conductor with a truncated Fourier series

$$E_z(\theta_p) = \sum_{n=-N_p}^{N_p} E_n^{(p)} e^{jn\theta_p}\,, \tag{1}$$

where $\theta_p \in [0, 2\pi]$.

Next, using the equivalence theorem from electromagnetics [12], MoM-SO replaces each conductor with the surrounding medium and an equivalent current distribution on its boundary. This step maintains the electric and magnetic fields outside the conductors unchanged, which will allow us to calculate the cable impedance. The obtained configuration is depicted in the center panel of Fig. 1. The equivalent current density $J_s(\theta_p)$, which accounts for the presence of the p-th conductor, is also expressed in truncated Fourier series

$$J_s(\theta_p) = \frac{1}{2\pi a_p} \sum_{n=-N_p}^{N_p} J_n^{(p)} e^{jn\theta_p}\,, \tag{2}$$

where a_p is the radius of the conductor. The value of the equivalent current $J_s(\theta_p)$ is related to the electric field on the boundary (1) through the so-called surface admittance operator [13] which, in discretized form, reads

$$\mathbf{J} = \mathbf{Y}_s \mathbf{E}\,, \tag{3}$$

where $\mathbf{J}$ and $\mathbf{E}$ are vectors that contain all the Fourier coefficients of $J_s(\theta_p)$ and $E_z(\theta_p)$, respectively. The surface admittance matrix $\mathbf{Y}_s$ can be found analytically for solid [13], [6] and hollow [7] round conductors. The surface admittance relation (3) fully describes, from an external viewpoint, the electromagnetic behavior of the conductor. Owing to this relation, MoM-SO can calculate the cable parameters by taking as unknowns only the electric field (1) on the boundary of the conductors. Since the region inside the conductors is not meshed, a large number of unknowns are saved with respect to conductor partitioning or the FEM, which translates into huge computational savings.

The equivalence theorem is applied a second time to further simplify the calculation of the cable parameters. The hole and the equivalent currents representing the conductors are replaced by a *single* equivalent current distribution $\widehat{J}_s(\hat{\theta})$ placed on the surface of the hole and by the surrounding medium [8]. This step transforms the configuration in the center panel of Fig. 1 into the configuration shown in the right panel of the same figure. The equivalent current $\widehat{J}_s(\hat{\theta})$ introduced on the boundary describes, in a very compact and efficient way, the hole and all conductors present inside. The equivalent current $\widehat{J}_s(\hat{\theta})$ satisfies a surface admittance relationship analogous to (3)

$$\widehat{\mathbf{J}} = \widehat{\mathbf{Y}}_s \widehat{\mathbf{A}} + \mathbf{T}\mathbf{J}\,, \tag{4}$$

as shown in [8]. In (4), $\widehat{\mathbf{J}}$ is the vector of Fourier coefficients of $\widehat{J}_s(\hat{\theta})$, and $\widehat{\mathbf{A}}$ is the vector of Fourier coefficients of the vector potential on the boundary of the hole. The two transformations turned a highly inhomogeneous electromagnetic problem (left panel of Fig. 1), into a much simpler problem where the surrounding medium is homogeneous in the x direction (right panel of Fig. 1). This step greatly facilitates the calculation of the cable parameters.

At this point, we can solve for the vector potential $\widehat{\mathcal{A}}_z$ on the boundary of the hole by applying the vector potential integral equation [14]

$$\widehat{\mathcal{A}}_z(\hat{\theta}) = -\mu_0 \int_0^{2\pi} \widehat{J}_s(\hat{\theta}) G_g(\hat{\theta}, \hat{\theta}') \hat{a} d\theta'\,, \tag{5}$$

where $\hat{a}$ is the radius of the hole and G_g is the Green's function of a two-layer medium [15], in our case the air-ground medium shown in the right panel of Fig. 1. Equation (5) provides a second relation between the equivalent current $\widehat{J}_s(\hat{\theta})$ and the fields. Combined with (4), equation (5) can be used to compute the vector potential on the boundary of the hole and the electric field $E_z(\theta_p)$ on the boundary of all conductors. Finally, the cable resistance and inductance can be readily obtained. The key conceptual steps behind the MoM-SO method, here briefly summarized, are described in detail in [6], [7], [8].

The main advantage of MoM-SO is that it provides the accuracy of a FEM analysis at a much lower computational cost. Its efficiency stems from the fact that MoM-SO does not require the discretization of the fields or currents inside the conductors, which would greatly increase complexity especially at high frequency, where the reduced skin depth imposes a very fine mesh near the conductor boundaries. The efficiency of MoM-SO allows for the computation of the resistance and inductance of complex power cables in a few seconds instead of the minutes or hours that a FEM analysis can take. This feature makes it ideal for the proposed study, where numerous cable configurations will be analysed.

III. Proximity Effects in Single-Core Cables in Flat Formation

In this section, we investigate the relevance of proximity effects on single-core (SC) cables laid in flat formation.

A. Simulation Setup

The configuration that we consider is shown in Fig. 2. Three single-core cables are buried at a depth of 1 m in a soil with conductivity $\sigma_g = 0.01$ S/m. The geometrical and material properties of each SC cable are presented in Table I. The spacing S between the SC cables will be varied from $S = 0$ to $S = 6D$, where D is the diameter of the cables.

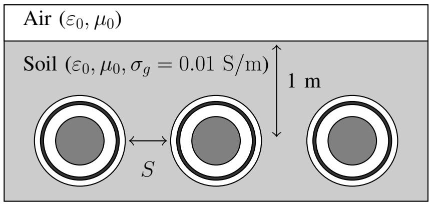

Fig. 2. The system of three SC cables considered in Sec. III. The separation between adjacent cable is denoted by S. In this figure, the conductive materials are shown in gray, while insulators are shown in white.

TABLE I
GEOMETRICAL AND MATERIAL PARAMETERS OF THE SINGLE-CORE CABLES CONSIDERED IN SEC. III

Core	Outer diameter = 39 mm, $\rho = 3.365 \cdot 10^{-8}\ \Omega \cdot \mathrm{m}$
Insulation	$t = 18.25$ mm, $\epsilon_r = 2.85$
Sheath	$t = 0.22$ mm, $\rho = 1.718 \cdot 10^{-8}\ \Omega \cdot \mathrm{m}$
Jacket	$t = 4.53$ mm, $\epsilon_r = 2.51$

In order to investigate the relevance of proximity effects, we computed the cable impedance using both MoM-SO, which accounts for proximity, and with standard analytic formulas [1], [16], which neglect proximity. The impedance values were calculated at 101 logarithmically-spaced points from 0.5 Hz to 1 MHz. The cable admittance was calculated using standard analytic formulas [1]. The calculated impedance and admittance parameters were then used to create two universal line models (ULMs) [17] and perform transient simulations.

B. Core Excitation

We first consider the scenario where the core conductor of the first cable is excited with a step voltage. The schematic of the circuit considered in this section is shown in Fig. 3. We consider the case where screens are grounded at one end, since, when screens are grounded are both ends, proximity effects are quite small. Grounding at both ends reduces proximity effects, but also reduces transmission capacity due to the thermal heating caused by the current flowing through the screens [18], [19].

Figure 4 shows the voltage of the first core conductor at the receiving end of the cable when cables are tightly-packed ($S = 0$), and when cables are far apart ($S = 4D$). In both cases, there is a very good agreement between the transient results obtained with and without accounting for proximity.

Proximity effects have instead a strong influence on the core voltage of the other conductors, and on sheath voltages.

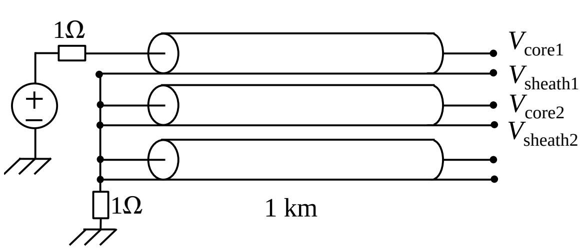

Fig. 3. Circuit schematic of the configuration considered in Sec. III-B. Screens are grounded at the source end.

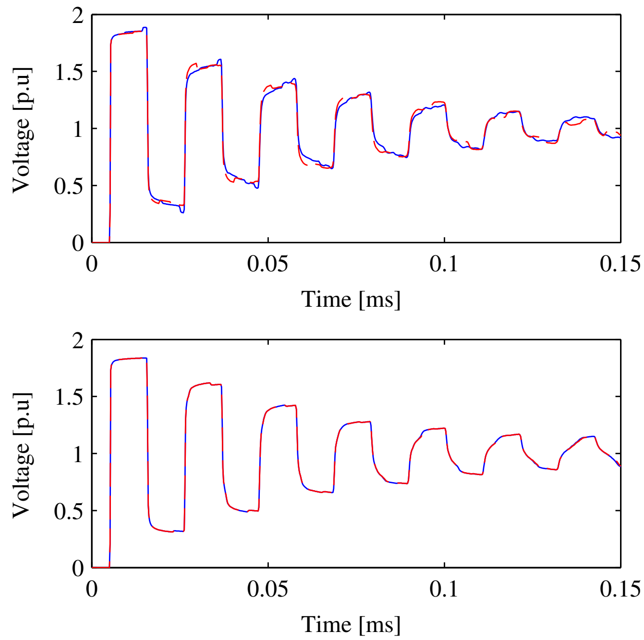

Fig. 4. Voltage V_{core1} of the first core conductor for the example of Sec. III-B, for a cable separation of $S = 0$ (top panel) and $S = 4D$ (bottom panel). The plots show the results obtained with proximity effects (—), and without proximity effects (- -).

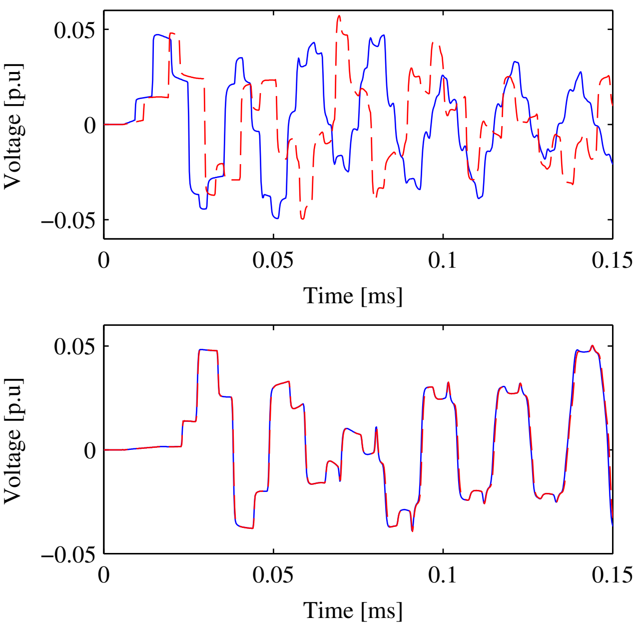

Fig. 5. Voltage $V_{sheath1}$ of the first sheath conductor for the example of Sec. III-B, for a cable separation of $S = 0$ (top panel) and $S = 4D$ (bottom panel). The plots show the results obtained with proximity effects (—), and without proximity effects (- -).

Figure 5 shows the voltage of the first sheath conductor $V_{sheath1}$ at the receiving end of the cable for $S = 0$ and $S = 4D$. This figure demonstrates that proximity effects significantly affect sheath voltages when cables are close to each other.

In order to understand for which separation proximity effects can be safely neglected, we performed a parametric

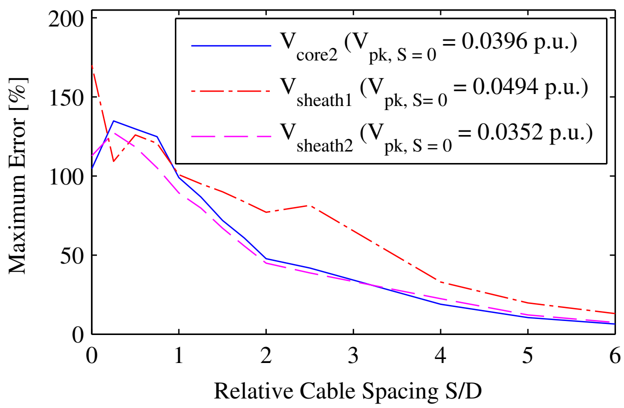

Fig. 6. Maximum error in transient voltages for the example considered in Sec. III-B. The peak voltage for each quantity is presented in the legend for the case of $S = 0$.

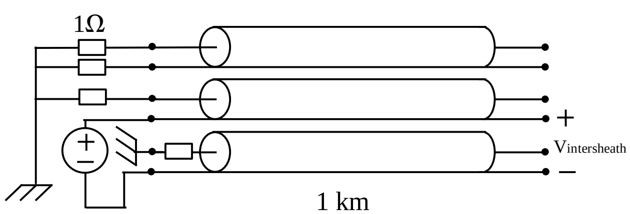

Fig. 7. Circuit schematic for the example of intersheath excitation considered in Sec. III-C.

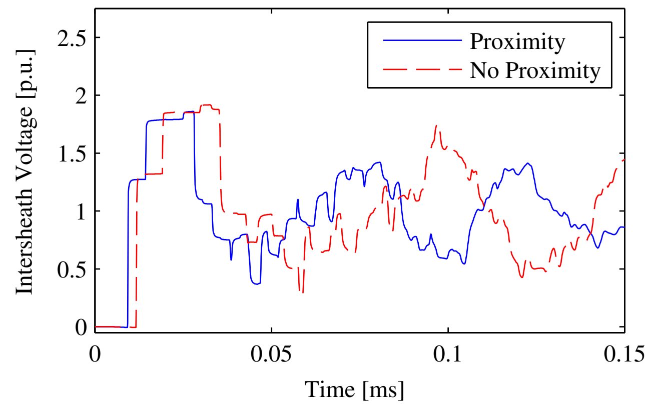

Fig. 8. Intersheath voltage at the receiving end of the transmission line in the example considered in Sec. III-C. The separation between the cables is $S = 0$.

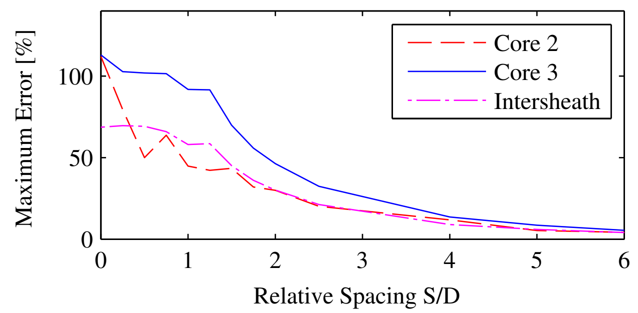

Fig. 9. Maximum error in transient voltages for the example in Sec. III-C, as a function of cables spacing.

transient analysis where the spacing between the cables is varied from $S = 0$ up to $S = 6D$. The transient voltages on the core and sheath conductors were computed for different cable spacings with and without proximity effects. The maximum relative error between the results obtained with and without accounting for proximity was then calculated as

$$\text{Maximum Error} = \max_t \left| \frac{V_{\text{prox}}(t) - V_{\text{no prox}}(t)}{\max_t |V_{\text{no prox}}(t)|} \right| \times 100\% \,. \quad (6)$$

Figure 6 depicts the maximum error on the voltages V_{core2}, $V_{sheath1}$, and $V_{sheath2}$. The figure demonstrates that neglecting proximity can result in transient errors beyond 100% when cables spacing S is comparable or smaller than the diameter of the cables. Error decays, as expected, as spacing S increases. Only when cable spacing S becomes larger than 6 times the diameter of the cables, proximity can be safely neglected without incurring large errors on the transient results.

C. Intersheath Excitation

Next, we consider a unit step excitation applied between the two sheaths. This test is useful to illustrate how proximity influences the propagation of the so-called intersheath mode. The circuit schematic for this setup is shown in Fig. 7. Figure 8 shows how proximity effects affect quite significantly the intersheath voltage at the receiving end of the cable when cables are close to each other. In Fig. 9, we present the maximum error on the transient results obtained for this setup when proximity is neglected, as a function of cables spacing S. The error is depicted for two core voltages, and for the intersheath voltage. Also in this case we observe that neglecting proximity is not an option when cables spacing is comparable to the cable diameter. Analytic formulas that neglect proximity can be used without a significant loss of accuracy only when cable spacing is greater than 3–4 times the cable diameter. In such case, neglecting proximity results in errors below 20% to 30% for core and intersheath voltages.

D. Power Loss

Finally, we show how neglecting proximity can affect the estimation of the power dissipated in the cable. Proximity effects increase eddy currents inside the conductors, which in turn increase power losses. We calculated the total power lost on the cable assuming a 3-phase sinusoidal excitation at 60 Hz. The relative error between the power calculated with and without proximity effects was then obtained as

$$\text{PL Error} = \frac{\text{PL}_{\text{prox}} - \text{PL}_{\text{no prox}}}{\text{PL}_{\text{no prox}}} \times 100\% \,. \quad (7)$$

Figure 10 shows this error for different values of cable spacing. The plot shows that neglecting proximity effects can result in an underestimation of power losses as large as 20% for low cable spacings. Error is depicted for three different values of the conductivity of the conductors, and is slightly higher when conductivity is larger.

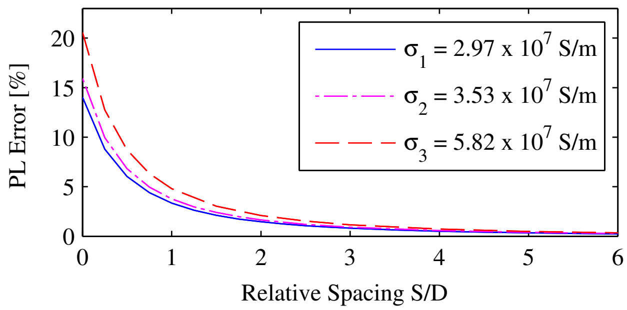

Fig. 10. Error on the power loss (7) at 60 Hz for the assembly of three SC cables considered in Sec. III-D.

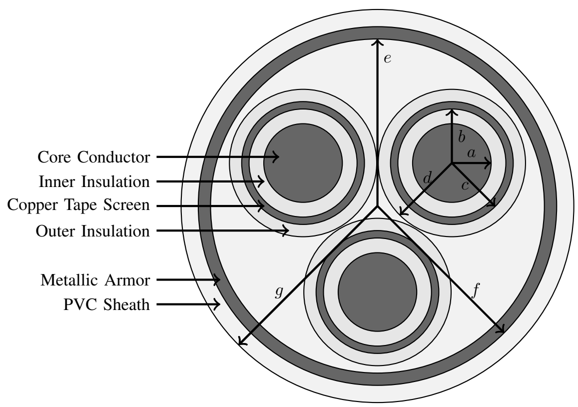

Fig. 11. Geometry of the pipe-type cable considered in Sec. IV.

IV. Proximity Effects in Pipe-Type Cables

We now investigate proximity effects in pipe-type cables made by three SC cables enclosed by a metallic armor. The cross-section of this type of cable is shown in Fig. 11. We consider a set of medium-voltage cables with rated voltage of 11 kV and different current ratings. All cables are compliant with the BS6622 cable standard [20]. The geometrical parameters and rated currents for each cable are listed in Table III. The geometrical parameters a, b, c, d, e, f, and g are defined in Fig. 11. The material properties of these cables are given in Table II. Cables are assumed to be 1 km long and buried at a depth of 1 m into a soil with conductivity $\sigma_g = 0.01$ S/m.

The SC cables inside the pipe are tightly packed, and significant proximity effects are expected. This is confirmed by Figure 12, which shows the current density inside the cable computed with MoM-SO at 600 Hz, with and without proximity effects. Neglecting proximity clearly changes the prediction of the current distribution in the core conductors, and results in no current flowing in the armor, as shown in the right panel of Fig. 12. The left panel of Fig. 12 depicts the correct current distribution obtained with MoM-SO. The plot shows that, as a result of proximity, an induced current will flow in the armor and contribute to power losses.

As in the previous section, the per-unit-length impedance of the cable was computed with MoM-SO, which accounts for proximity, and with standard analytic formulas [1], [16], which neglect proximity. The cable admittance was computed with standard analytic formulas [1]. The calculated parameters were then used to create two ULM models [17] for each cable, and perform transient analyses.

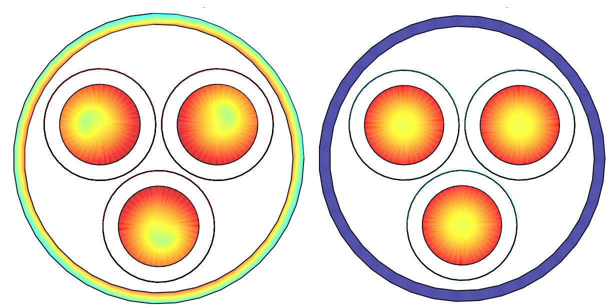

Fig. 12. Current density inside the pipe-type cable of Sec. IV with proximity (left panel) and without proximity (right panel). These plots were computed with MoM-SO at 600 Hz when a 3-phase excitation was applied on the core conductors.

TABLE II
Material Parameters of the Pipe-Type Cable Considered in Sec. IV

Core Conductor	$\sigma = 5.8 \cdot 10^7$ S/m
Inner Insulation	$\varepsilon_r = 2.3$
Metallic Copper tape Screen	$\sigma = 5.8 \cdot 10^7$ S/m
Outer Insulation	$\varepsilon_r = 2.3$
Metallic Armor	$\sigma = 5.56 \cdot 10^6$ S/m, $\mu_r = 100$
PVC Sheath	$\varepsilon_r = 3$

TABLE III
Three-Core Cable Dimensions Considered for the Example in Sec. IV

#	a	b	c	d	e	f	g	I_{max}
1	4.90	8.90	9.00	9.50	22.5	25.0	27.8	195
2	5.75	9.75	9.85	10.35	24.5	27.0	29.8	230
3	6.40	10.40	10.50	11.00	26.0	28.8	31.6	265
4	7.15	11.15	11.25	11.75	27.7	30.5	33.3	300
5	7.95	11.95	12.05	12.55	29.7	32.5	35.3	335
6	9.20	13.20	13.30	13.80	32.5	35.3	38.8	380
7	10.25	14.45	14.55	15.05	35.1	38.3	41.3	435
8	11.60	16.00	16.10	16.60	38.6	41.8	45.3	490

Note: All units in columns 2-8 are in mm.
Column 9 presents rated current in Amperes.

A. Core Excitation

The core conductor of the SC cable was excited with a unit step voltage, with sheaths and armor grounded at the source end. The circuit schematic for this setup is the same as the one in Fig. 3, with in addition the armor conductor grounded at the source end. First, we look at the error (6) that arises on transient results if proximity is neglected. Fig. 13 plots the maximum error on the voltage V_{core1} as a function of the normalized core radius a/d, where a is the radius of the core conductor, and d is the outer radius of the whole SC cable, as depicted in Fig. 11. The error is relatively low for all cases, and increases mildly as the core radius increases. The error on the voltages of another core conductor and on the sheaths is instead much larger, as shown by Fig. 14. For all cables, which have different core radii, neglecting proximity results in relative errors beyond 100%. The error depends on the normalized core radius a/d, but a monotonic dependence cannot be identified. These results

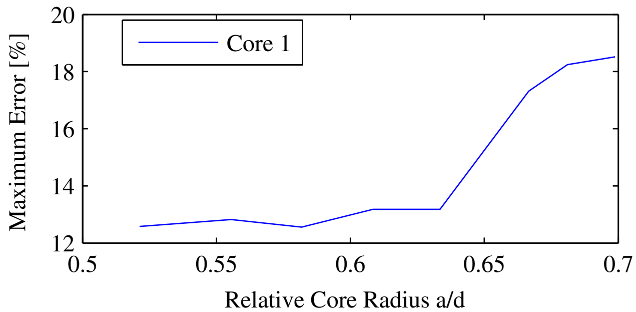

Fig. 13. Maximum error in core 1 transient voltage for the example considered in Sec. IV-A.

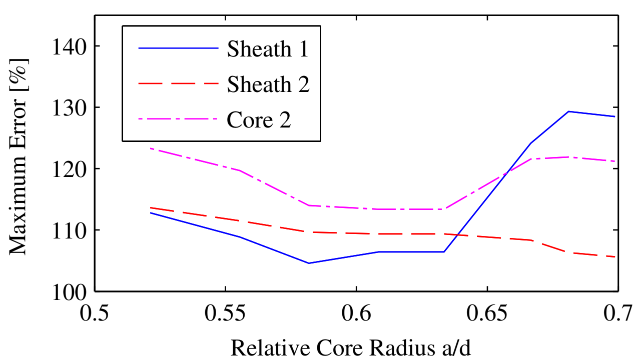

Fig. 14. Maximum error in core 2, sheath 1 and 2 transient voltages for the example considered in Sec. IV-A.

show how that the significance of proximity effects for pipe-type cables cannot be easily estimated a priori, due to the complex geometry of the cable.

B. Intersheath Excitation

We now repeat the analysis considering a unit step excitation applied between two sheaths. The circuit schematic for this test is as in Fig. 7, with in addition the cable armor grounded at the source end. Figure 15 shows the error on the transient voltages (6) for different core voltages, and for the intersheath voltage. Even though the transient voltages of cores 2 and 3 are different, the maximum error variation for both of them is identical, due to the symmetry in the cable geometry. The results in Fig. 15 show that the maximum error without proximity can be higher than 100%, which is very significant. However, no clear relation can be observed between the error and the relative core radius of the cable.

C. Power Loss

The influence of proximity effects on power losses was estimated by applying a 3-phase 60-Hz sinusoidal excitation to the cable. The error on the power dissipated in the cable predicted with and without proximity effects was calculated with (7) and is depicted in Fig. 16. The error is larger for larger cores, and can exceed 30%.

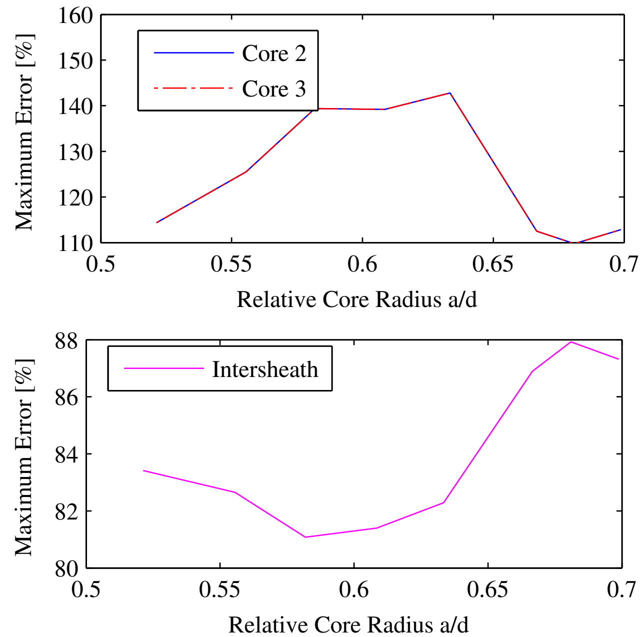

Fig. 15. Maximum error in core 2, core 3, and intersheath voltages for the example considered in Sec. IV-B.

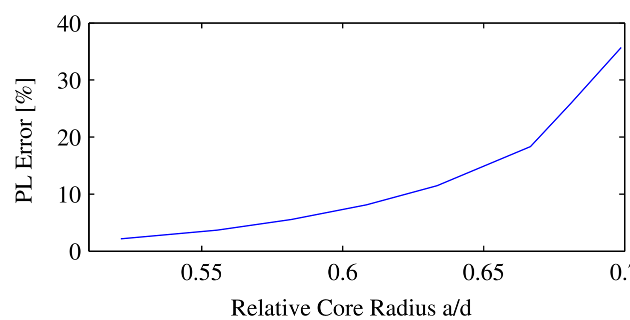

Fig. 16. Power loss error in eight different 3-core cables considered in Sec. IV-A. Each cables a/d ratio is used to generate the plot of normalized power loss vs. relative core radius.

V. Conclusion

In this paper, we presented a comprehensive investigation on the relevance of proximity effects on underground power cables. Both single-core cables in flat formation and pipe-type cables were considered. The influence of proximity effects on transient voltages and power losses was analyzed as a function of the cable geometry and of the type of excitation applied to the cable. The obtained results can be summarized as follows. For cables in flat formation under core excitation, neglecting proximity can induce fairly large errors on the prediction of core and sheath voltages. Errors can exceed 100% when cables are very close to each other, and can be neglected only when spacing is higher than 5–6 times their diameter. Comparable errors arise in the prediction of the transient voltages caused by an intersheath excitation. Neglecting proximity also leads to an underestimation of the total power dissipated on the cable under nominal 3-phase AC operation. The underestimation can be as large as 20% for closely-space cables. In pipe-type cables, proximity effects are very significant, since conductors are tightly packed. Neglecting proximity can produce transient errors in excess of 100% and errors on the dissipated power as high as 30%. In this case, however, it is harder to correlate the significance of proximity effects to the cable geometry. In conclusion, this study provides further evidence that, in several transient scenarios, proximity effects have a significant influence on transient voltages. Therefore, in order to obtain accurate predictions, proximity must be accurately taken into account when computing cable parameters for the simulation of electromagnetic transients in power cables.

REFERENCES

[1] A. Ametani, “A general formulation of impedance and admittance of cables,” *IEEE Trans. Power App. Syst.*, no. 3, pp. 902–910, 1980.

[2] B. Gustavsen, J. Sletbak, and T. Henriksen, “Simulation of transient sheath overvoltages in the presence of proximity effects,” *IEEE Trans. Power Del.*, vol. 10, pp. 1066–1075, April 1995.

[3] U. S. Gudmundsdottir, B. Gustavsen, C. L. Bak and W. Wiechowski, “Field test and simulation of a 400-kv cross-bonded cable system,” *IEEE Trans. Power Del.*, vol. 26, no. 3, pp. 1403 –1410, 2011.

[4] U. R. Patel, B. Gustavsen, and P. Triverio, “Application of the MoM-SO Method for Accurate Impedance Calculation of Single-Core Cables Enclosed by a Conducting Pipe,” in *10th International Conference on Power Systems Transients (IPST 2013)*, Vancouver, Canada, July 18–20 2013.

[5] U. S. Gudmundsdottir, “Proximity ffect in fast transient simulations of an underground transmission cable,” *Electric Power Systems Research*, vol. 115, pp. 50–56, Oct. 2014.

[6] U. R. Patel, B. Gustavsen, and P. Triverio, “An Equivalent Surface Current Approach for the Computation of the Series Impedance of Power Cables with Inclusion of Skin and Proximity Effects,” *IEEE Trans. Power Del.*, vol. 28, pp. 2474–2482, 2013.

[7] ——, “Proximity-Aware Calculation of Cable Series Impedance for Systems of Solid and Hollow Conductors,” *IEEE Trans. Power Delivery*, vol. 29, no. 5, pp. 2101–2109, Oct. 2014.

[8] U. R. Patel and P. Triverio, “MoM-SO: a Complete Method for Computing the Impedance of Cable Systems Including Skin, Proximity, and Ground Return Effects,” *IEEE Trans. Power Del.*, 2014, (in press).

[9] B. Gustavsen, A. Bruaset, J. Bremnes, and A. Hassel, “A finite element approach for calculating electrical parameters of umbilical cables,” *IEEE Trans. Power Del.*, vol. 24, no. 4, pp. 2375–2384, Oct. 2009.

[10] A. Pagnetti, A. Xemard, F. Paladian and C. A. Nucci, “An improved method for the calculation of the internal impedances of solid and hollow conductors with the inclusion of proximity effect,” *IEEE Trans. Power Del.*, vol. 27, no. 4, pp. 2063 –2072, Oct. 2012.

[11] COMSOL Multiphysics. COMSOL, Inc. [Online]. Available: https://www.comsol.com/

[12] C. A. Balanis, *Antenna Theory: Analysis and Design*, 3rd ed. Wiley, 2005.

[13] D. De Zutter, and L. Knockaert, “Skin Effect Modeling Based on a Differential Surface Admittance Operator,” *IEEE Trans. Microw. Theory Tech.*, vol. 53, no. 8, pp. 2526 – 2538, Aug. 2005.

[14] R. F. Harrington, *Time-Harmonic Electromagnetic Fields*. McGraw-Hill, 1961.

[15] C. A. Balanis, *Advanced Engineering Electromagnetics*. John Wiley & Sons, 1989.

[16] L.M. Wedephol, and D.J. Wilcox, “Transient analysis of underground power-transmission systems. System-model and wave-propagation characteristics,” *Proc. IEEE*, vol. 120, no. 2, pp. 253–260, Feb. 1973.

[17] A. Morched, B. Gustavsen, M. Tartibi, “A universal model for accurate calculation of electromagnetic transients on overhead lines and underground cables,” *IEEE Trans. Power Del.*, vol. 14, no. 3, pp. 1032–1038, 1999.

[18] F. F. Da Silva and C. L. Bak, *Electromagnetic Transients in Power Cables*. Springer, 2013.

[19] J. Martinez-Velasco, *Power System Transients. Parameter Determination*. CRC Press, 2010.

[20] Nexans, “6-36kv medium voltage underground power cables,” 2015, www.nexans.com.